

# Aminomethylene Peptide Nucleic Acid (*am*-PNA): Synthesis, Regio-/Stereospecific DNA Binding, And Differential Cell Uptake of ( $\alpha/\gamma,R/S$ )*am*-PNA Analogues

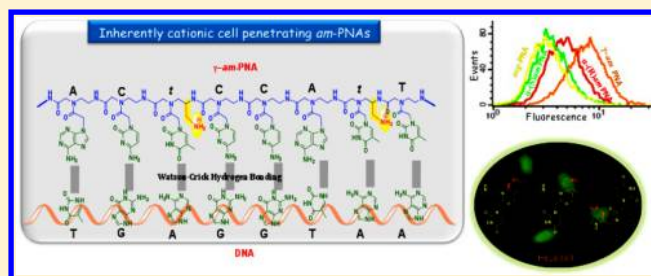
Roopa Mitra<sup>†</sup> and Krishna N. Ganesh<sup>\*,†,‡</sup>

<sup>†</sup>Organic Chemistry Division, National Chemical Laboratory, Pune 411008, India

<sup>‡</sup>Indian Institute of Science Education and Research, 900, NCL Innovation Park, Dr Homi Bhabha Road, Pune 411008, India

## S Supporting Information

**ABSTRACT:** Inherently chiral, cationic *am*-PNAs having pendant aminomethylene groups at  $\alpha(R/S)$  or  $\gamma(S)$  sites on PNA backbone have been synthesized. The modified PNAs are shown to stabilize duplexes with complementary cDNA in a regio- and stereo-preferred manner with  $\gamma(S)$ -*am* PNA superior to  $\alpha(R/S)$ -*am* PNAs and  $\alpha(R)$ -*am* PNA better than the  $\alpha(S)$  isomer. The enhanced stabilization of *am*-PNA:DNA duplexes is accompanied by a greater discrimination of mismatched bases. This seems to be a combined result of both electrostatic interactions and conformational preorganization of backbone favoring the cDNA binding. The *am*-PNAs are demonstrated to effectively traverse the cell membrane, localize in the nucleus of HeLa cells, and exhibit low toxicity to cells.



## INTRODUCTION

Peptide nucleic acids (PNAs) are a promising class of oligonucleotide analogues with great potential for gene therapeutic applications.<sup>1</sup> They are effective DNA mimics with a structurally homomorphous pseudopeptide backbone composed of achiral *N*-(2-aminoethyl)glycine (*aeg*) units to which a nucleobase (A, C, T, or G) is attached via a methylene carbonyl linker (Figure 1a).<sup>2</sup> The neutral backbone of PNA

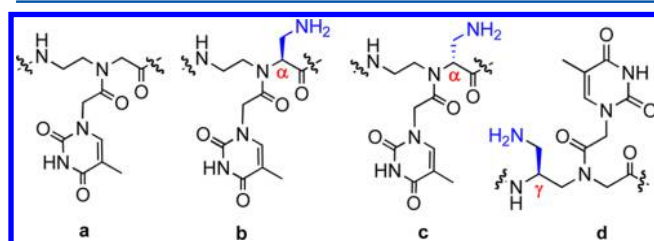


**Figure 1.** Chemical structures of (a) *aeg* PNA, (b) and (c)  $\alpha$ -*am*, and (d)  $\gamma$ -*am* PNA.

offers an advantage for hybridizing the negatively charged cDNA and RNA with high affinity mediated by Watson–Crick base pairing. The unnatural polyamide linkage makes it resistant to degradation by both proteases and nucleases.<sup>3</sup> The simple structure in combination with its impressive properties and ease of synthesis has made PNA attractive as a putative gene regulatory agent.<sup>4–6</sup> However, in order to be used as an efficacious antigene or antisense drug, it must be able to traverse efficiently into the cells. Despite its remarkable properties, the major challenges that *aeg* PNA face are its low

aqueous solubility, ambiguity in directional (parallel/antiparallel) selectivity of binding cDNA/RNA, and refractory for taking up by mammalian cells.<sup>7</sup> Several modified PNA analogues have been rationally designed and synthesized in order to overcome some of the limitations.<sup>8–10</sup>

As compared to many negatively charged analogues, neutral *aeg* PNA hybridizes to cDNA/RNA targets with a greater affinity and without loss of specificity.<sup>11</sup> Incorporation of positive charge in PNA variants through incorporation of *N*-(2-aminoethyl)-*D*-lysine units has shown some advantages in terms of improved solubility and efficient binding to cDNA.<sup>9,10</sup> The crystal structure of a PNA–DNA decamer heteroduplex, comprising three residues of aminoethyl-*D*-lysine on the PNA backbone, has indicated that the presence of chirality may conformationally tune the PNA backbone by influencing the helical direction and thereby improving the recognition specificity of the cDNA, and the positive charge enhances the solubility and bioavailability to bind the DNA targets.<sup>12,13</sup> Recently, promising evidence was seen with cationic guanidinium PNAs (GPNA) of appropriate backbone stereochemistry that bind sequence specifically to RNA and traverse the cell membrane readily.<sup>14</sup> The X-ray structure of *D*-lysine-based PNA revealed that the oxygen atom of the backbone >C=O group is within a  $3.17 \pm 0.1$  Å vicinity of the  $\gamma$ -carbon of *D*-lysine side chain.<sup>15</sup> This suggested that a shortening of the aliphatic chain by removal of the three methylene carbons may permit a direct interaction of side chain NH<sub>2</sub> group with the

Received: April 29, 2012

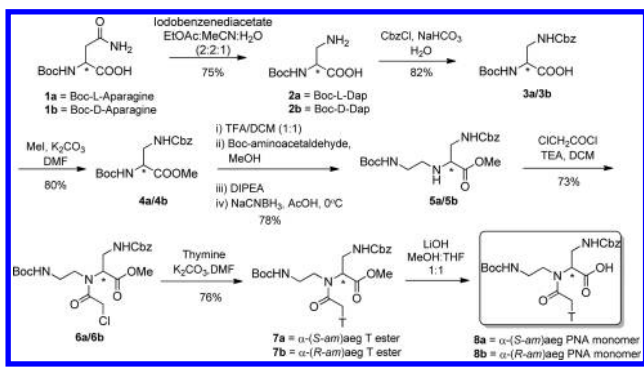
Published: June 7, 2012

carbonyl oxygen of amide backbone of PNA. Quantum-mechanical studies by Topham et al.<sup>16</sup> supported such an idea of the hydrogen bonding of the protonated side chain methylene amino group with the carbonyl of the polyamide backbone. Based on this hypothesis, we showed in a recent communication that synthetic PNA constructs with a chiral backbone bearing cationic aminomethylene (*am*) side-chain substitution (Figure 1b–d) exhibit improved cDNA hybridization properties.<sup>17</sup> Herein we report the detailed synthesis and hybridization studies of mono- and disubstituted aminoethyl- $\alpha$ -(*S*-aminomethylene)glycine PNA [ $\alpha$ -(*S*-*am*) PNA] (Figure 1b) and aminoethyl- $\alpha$ -(*R*-aminomethylene)glycine PNA [ $\alpha$ -(*R*-*am*) PNA] (Figure 1c). We observe a stereo-preferred enhancement in the binding of  $\alpha$ -(*R*-*am*) PNA with cDNA and higher cell permeability of *am*-PNAs accompanied by a low toxicity for cells. The  $\gamma$ -position is a hot spot for modifications as shown recently in  $\gamma$ -substituted L-lysine PNAs, which had favorable DNA hybridization properties.<sup>18–21</sup> The presence of  $\gamma$ -(*S*)-substituent (derived from appropriate L-amino acids) induces conformational preorganization of randomly folded PNA into a right handed helix.<sup>22–24</sup> In this context, we also report the synthesis, biophysical, and cell uptake studies of  $\gamma$ -(*S*-aminomethylene)aminoethylglycyl PNA [ $\gamma$ -(*S*-*am*) PNA] (Figure 1d), which was found to be superior to  $\alpha$ -(*R*/*S*-*am*) PNA analogues.

## RESULTS AND DISCUSSION

**Synthesis of *am*-PNA Monomers.** The synthesis of designed PNA-T monomers,  $\alpha$ -(*S*/*R*-*am*) (**8a,b**) and  $\gamma$ -(*S*-*am*) (**16**), was performed starting with the conversion of *N*-Boc-asparagine **1** to *N* $\alpha$ -Boc-diaminopropionic acid **2** via Curtius rearrangement,<sup>25,26</sup> followed by orthogonal protection of the side chain amine with Cbz (Scheme 1). The acid was

**Scheme 1. Synthesis of  $\alpha$ -*am*-PNA Monomers**



converted into its ester **4**, which became the common precursor for the synthesis of all target monomers. In order to synthesize  $\alpha$ -(*S*/*R*-*am*) PNA-T monomers **8a** and **8b**, the *N*1-Boc group in compound **4** was deprotected and the resultant amine was reacted with *N*-Boc-aminoacetaldehyde<sup>27</sup> to a Schiff base which was in situ reduced with  $\text{NaBH}_3\text{CN}$  and acetic acid. The resulting *N*-protected *S*-(*am*) (**5a**) and *R*-(*am*) (**5b**) having a side-chain substituent at the  $\alpha$ -carbon were obtained in good yields. These were acylated with chloroacetyl chloride to obtain **6a** and **6b**, respectively, which were used for alkylation of thymine at N-1 to yield the corresponding esters **7a** and **7b** in quantitative yields. The esters on hydrolysis gave the target PNA-T monomers *N*-Boc- $\alpha$ -(*S*-*am*) **8a** and *N*-Boc- $\alpha$ -(*R*-*am*) **8b**, respectively. The optical purities of the monomers **8a** and

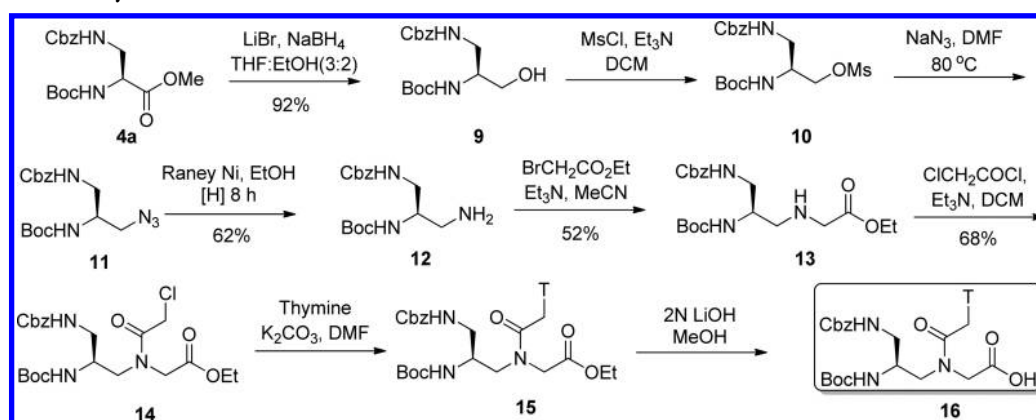
**8b** were determined by  $^{19}\text{F}$  NMR of the corresponding Mosher esters,<sup>28,29</sup> and **8a/8b** were used for the solid-phase synthesis of ( $\alpha$ )-(*R*/*S*-*am*) PNA oligomers **P2–P7**.

Similarly, the synthesis of  $\gamma$ -(*S*-*am*) PNA-T monomer **16** (Scheme 2) was attempted starting from compound **4a**, which was reduced to the corresponding alcohol **9** followed by conversion to *O*-mesyl derivative **10**. This was treated with  $\text{NaN}_3$  to obtain the azido derivative **11** that was hydrogenated to the amine **12**. It was alkylated with ethyl bromoacetate to **13**, followed by *N*-acylation with chloroacetyl chloride to **14** and subsequent reaction with thymine to obtain the ester **15**. The hydrolysis of the ester with  $\text{LiOH}$  afforded the  $\gamma$ -(*S*-*am*) PNA-T monomer **16** that was used for the synthesis of  $\gamma$ -(*S*-*am*) PNA oligomers **P8–P10**. All intermediate compounds and the final monomers were characterized by  $^1\text{H}$ ,  $^{13}\text{C}$  NMR and mass spectroscopic data (see the Supporting Information).

**Synthesis of *am*-PNA Oligomers.** The modified *am*-PNA-T monomers (**8a**, **8b**, and **16**) were incorporated at predefined sites within the *aeg* PNA mixed-oligomer sequence **P1** on the solid phase using Boc chemistry on L-lysine-derivatized MBHA resin using the standard protocol. The synthesis was carried out using HOBt–HBTU–DIPEA as coupling reagent. The deprotection of the Cbz protecting group on the side-chain amine was achieved synchronously during the final step of cleavage of the peptide from the resin using TFA–TFMSA. The different mixed purine–pyrimidine decamers that were synthesized are listed in Table 1 with the site of incorporation of modified T-monomers denoted by  $t^{(S)}$  (**P2–P4**),  $t^{(R)}$  (**P5–P7**), and  $t'$  (**P8–P10**). The fluorescent PNA analogues (*cfP1*, *cfP4*, *cfP7*, and *cfP10*) required for monitoring the cell uptake were synthesized by coupling the corresponding PNA oligomers on the solid phase at the N-terminus with 5/6-carboxyfluorescein succinimidyl ester before cleavage from the resin. All PNA oligomers were purified by reverse-phase HPLC, and their final purity was checked on analytical RP-HPLC (C-18). The integrity of all PNA oligomers was confirmed by MALDI-TOF data (see the Supporting Information).

**Stoichiometry of *am*-PNA:DNA Hybrids.** Although the  $\alpha$ -(*R*/*S*-*am*) PNAs have a chiral-center, single-stranded PNA with even the double modification did not show any appreciable CD signals (Figure 2). In contrast, the doubly modified  $\gamma$ -(*S*-*am*) PNA (**P10**) exhibited negative CD signal at 273 nm suggesting a base-stacked helical preorganization present in the  $\gamma$ -(*S*-*am*)-PNA oligomers. However, upon binding with cDNA, all PNAs show strong CD signals whose intensity can be used for monitoring the strength of binding. The binding stoichiometry of *am*-PNA:DNA complexation was established by a Job's plot using CD data (ellipticity at 262 nm) and confirmed by UV data (absorbance at 260 nm) to be 1:1 (Supporting Information).

**PNA:DNA Hybridization Studies.** To assess the impact of grafting the aminomethylene group on the PNA backbone on the stability of PNA:DNA duplexes, the synthesized *am*-PNAs (**P1–P10**) were individually annealed with the cDNAs [DNA1, antiparallel duplex, PNA (N  $\rightarrow$  C):DNA1 (3'–5') and DNA2, parallel duplex, PNA (N  $\rightarrow$  C):DNA2 (5'–3')], and the thermal stability  $T_m$  of the derived PNA:DNA duplexes was obtained by temperature-dependent UV-absorbance measurements. The results shown in Table 2 indicate that the cationic *am*-PNAs (**P2–P10**) formed much more stable duplexes than the unmodified PNA **P1**, with the binding affinity dependent on the position, stereochemistry, and the number of modifications.

Scheme 2. Synthesis of  $\gamma$ -*am*-PNA MonomerTable 1. PNA Oligomers Synthesized along with Their Molecular Weight<sup>a</sup>

S. no.	oligomers	sequence	calcd MW	obsd MW
P1	<i>aeg</i> PNA	H-TTACCTCAGT-LysNH <sub>2</sub>	2805.74	2805.06
P2	$\alpha$ -( <i>S-am</i> ) PNA	H-TTACCTCAG $\overset{\alpha(S)}{\text{T}}$ -LysNH <sub>2</sub>	2834.78	2834.78
P3	$\alpha$ -( <i>S-am</i> ) PNA	H-TTACC $\overset{\alpha(S)}{\text{T}}$ CAGT-LysNH <sub>2</sub>	2834.78	2831.17
P4	$\alpha$ -( <i>S-am</i> ) PNA	H-T $\overset{\alpha(S)}{\text{T}}$ A CC $\overset{\alpha(S)}{\text{T}}$ C AGT-Lys NH <sub>2</sub>	2863.82	2884.33 [M + Na <sup>+</sup> ]
P5	$\alpha$ -( <i>R-am</i> ) PNA	H-TTACCTCAG $\overset{\alpha(R)}{\text{T}}$ -LysNH <sub>2</sub>	2834.78	2833.01
P6	$\alpha$ -( <i>R-am</i> ) PNA	H-TTACC $\overset{\alpha(R)}{\text{T}}$ CAGT-LysNH <sub>2</sub>	2834.78	2834.20
P7	$\alpha$ -( <i>R-am</i> ) PNA	H-T $\overset{\alpha(R)}{\text{T}}$ ACC $\overset{\alpha(R)}{\text{T}}$ C AGT-LysNH <sub>2</sub>	2863.82	2885.18 [M + Na <sup>+</sup> ]
P8	$\gamma$ -( <i>S-am</i> ) PNA	H-TTACCTCAG $\overset{\gamma}{\text{T}}$ -LysNH <sub>2</sub>	2834.78	2834.21
P9	$\gamma$ -( <i>S-am</i> ) PNA	H-TTACC $\overset{\gamma}{\text{T}}$ CAGT-LysNH <sub>2</sub>	2834.78	2830.85
P10	$\gamma$ -( <i>S-am</i> ) PNA	H-T $\overset{\gamma}{\text{T}}$ ACC $\overset{\gamma}{\text{T}}$ CA GT-LysNH <sub>2</sub>	2863.82	2862.08
<i>cf</i> P1	<i>cf aeg</i> PNA	H- <i>cf</i> -TTACCTCAGT-LysNH <sub>2</sub>	3166.06	3185.83 [M + Na <sup>+</sup> ]
<i>cf</i> P4	<i>cf</i> $\alpha$ -( <i>S-am</i> ) PNA	H- <i>cf</i> -T $\overset{\alpha(S)}{\text{T}}$ ACC $\overset{\alpha(S)}{\text{T}}$ CAGT-LysNH <sub>2</sub>	3224.14	3242.67 [M + Na <sup>+</sup> ]
<i>cf</i> P7	<i>cf</i> $\alpha$ -( <i>R-am</i> ) PNA	H- <i>cf</i> -T $\overset{\alpha(R)}{\text{T}}$ ACC $\overset{\alpha(R)}{\text{T}}$ CAGT-LysNH <sub>2</sub>	3224.14	3222.29
<i>cf</i> P10	<i>cf</i> $\gamma$ -( <i>S-am</i> ) PNA	H- <i>cf</i> -T $\overset{\gamma}{\text{T}}$ ACC $\overset{\gamma}{\text{T}}$ CAGT-LysNH <sub>2</sub>	3224.14	3221.71

<sup>a</sup>See the Supporting Information for mass spectra.

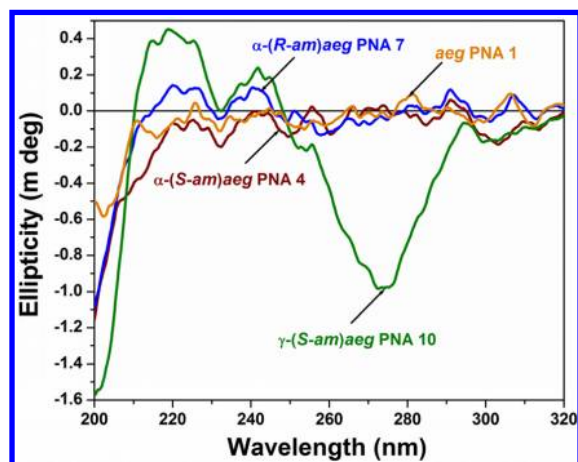


Figure 2. Comparison of CD spectra of unmodified *aeg* PNA with doubly modified  $\alpha$ -(*S-am*)*aeg*,  $\alpha$ -(*R-am*)*aeg*, and  $\gamma$ -(*S-am*)*aeg* PNA sequences. All samples were prepared in buffer containing 10 mM sodium phosphate and 10 mM NaCl at 2  $\mu$ M strand concentration each.

The comparative differential  $T_m$  ( $\Delta T_m$ ) calculated for the modified PNA oligomers P2–P10 in relation to unmodified PNA P1 and for the analogous antiparallel and parallel PNA:DNA duplex pairs are shown in Figure 3.

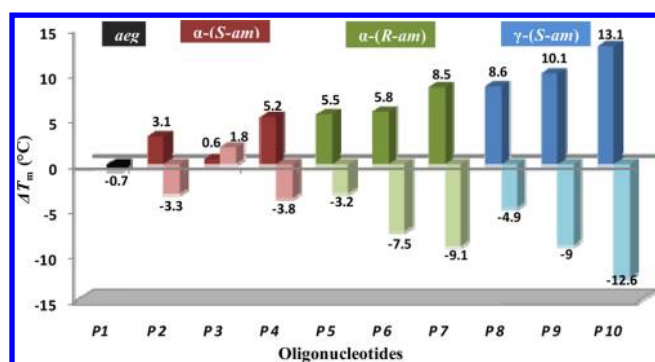
Among the  $\alpha$ -*am*-modifications, with reference to unmodified PNA P1,  $\alpha$ -(*R-am*) PNAs P5–P7 (entries 5–7) show

Table 2. UV- $T_m$  ( $^{\circ}$ C) Studies of  $\alpha$ -*am* and  $\gamma$ -*am* PNA/DNA Hybrids<sup>a</sup>

entry	oligomers	DNA1 ( <i>ap</i> )	DNA2 ( <i>p</i> )	DNA3 ( <i>mismatch</i> )
1	PNA 1	49.2	48.5	42.2
2	$\alpha$ -( <i>S-am</i> ) PNA 2	52.3	49.0	46.8
3	$\alpha$ -( <i>S-am</i> ) PNA 3	49.8	51.6	45.0
4	$\alpha$ -( <i>S-am</i> ) PNA 4	54.4	50.6	42.5
5	$\alpha$ -( <i>R-am</i> ) PNA 5	54.7	51.5	44.8
6	$\alpha$ -( <i>R-am</i> ) PNA 6	55.0	47.5	42.2
7	$\alpha$ -( <i>R-am</i> ) PNA 7	57.7	48.6	41.0
8	$\gamma$ -( <i>S-am</i> ) PNA 8	57.8	52.9	42.2
9	$\gamma$ -( <i>S-am</i> ) PNA 9	59.3	50.3	41.7
10	$\gamma$ -( <i>S-am</i> ) PNA 10	62.3	49.7	44.0

<sup>a</sup>DNA1 (*ap*; antiparallel) = 5'ACTGAGGTAA3'; DNA2 (*p*; parallel) = 5'AATGGAGTCA3'; DNA3 (with C:C base pair mismatch) = 5'ACTGCGGTAA3'.

substantial enhancement of duplex stability ( $\Delta T_m = +5.5$  to  $+8.5$   $^{\circ}$ C) with antiparallel DNA1 as compared to  $\alpha$ -(*S-am*) PNAs P2–P4 (entries 2–4) ( $\Delta T_m = +0.6$  to  $+5.2$   $^{\circ}$ C). The stabilization is least when the modification is in the middle of the sequence (P3). The degree of stabilization is also enhanced with an increase in the number of modifications (P2 and P4, 2.1 $^{\circ}$ /mod; P5 and P7, 2.8 $^{\circ}$ /mod). Interestingly, a single  $\gamma$ -modified PNA (P8, P9) had a more striking effect on the DNA-binding properties of PNA by stabilizing the duplex with antiparallel DNA1 ( $\Delta T_m = +8.6$  to  $+10$   $^{\circ}$ C) depending on the



**Figure 3.** Comparative  $\Delta T_m$  values for *aeg*-PNA P1,  $\alpha$ -(*S-am*) PNA P2–P4,  $\alpha$ -(*R-am*) PNA P5–P7, and  $\gamma$ -(*S-am*) PNA P8–P10 with complementary antiparallel DNA1, 5'ACTGAGGTAA3', and complementary parallel DNA2, 5'AATGGAGTCA3'. For each *am*-PNA, the darker shade represents the amount of stabilization over that with control ( $\Delta T_m = (T_m^{Pn} - T_m^{P1})$ ) for binding with DNA1 and the lighter shade represents  $\Delta T_m = T_m(p) - T_m(ap)$ .

position of modification, and with doubly modified PNAs, the stabilization of the duplex increased by 5°/mod (P8 and P10).

**Parallel vs Antiparallel Duplexes.** In order to evaluate the orientational selectivity of DNA binding in complementary antiparallel and parallel directions, UV melting studies were done using the parallel cDNA2 and the comparative data is shown in Figure 3 (represented by lighter shade). It reveals that duplexes of *am*-PNAs P2–P10 with cDNA2 are considerably less stable than the analogous antiparallel duplexes. The directional selectivity in binding is distinctly better in doubly modified  $\gamma$ -(*S-am*) PNA 10 where the parallel duplex is significantly destabilized ( $\Delta T_m = -12.6$  °C) with cDNA2 as compared to hybrid with antiparallel cDNA1 ( $\Delta T_m = +13$  °C). The stabilizing effects were always better in case of  $\alpha$ -(*R-am*) analogues compared to  $\alpha$ -(*S-am*) with the exception of the  $\alpha$ -(*S-am*) PNA3 having modification in the middle of the sequence wherein the derived parallel duplex with DNA2 was slightly more stable than the duplex with opposite stereomer  $\alpha$ -(*R-am*) PNA 6.

**Mismatched Duplexes.** The higher binding of cationic *am*-PNAs with anionic DNA could merely arise from favorable electrostatic interactions between the two backbones. Hence, to establish the sequence specificity of binding, the stability of antiparallel duplexes of *am*-PNAs with cDNA3 (Table 2) having a single C:C base-pair mismatch in the middle was measured. The introduction of one base-pair mismatch allowed the formation of duplexes but considerably destabilized the complexes (Figure 4). The duplexes exhibited considerable destabilization with  $\gamma$ -(*S-am*) PNAs P9 and P10 ( $\Delta T_m \approx -15$  to  $-18$  °C) followed by *R*-(*am*) PNAs P5–P7 ( $\Delta T_m \approx -10$  to  $-16$  °C), *S*-(*am*) PNAs P2–P4 ( $\Delta T_m \approx -5$  to  $-12$  °C), and the unmodified PNA P1 ( $\Delta T_m \approx -7$  °C). The destabilization from mismatch was higher than the stabilization gained due to *am*-modifications, clearly suggesting that the higher binding affinity of the cationic *am*-PNAs (P2–P10) with anionic DNA was achieved without compromising the base specificity. Both the regio- ( $\alpha/\gamma$ ) and stereospecificity (*S/R*) of aminomethylene side chains are important determinants in defining the stability of derived PNA:DNA duplexes.

**Cellular Uptake of *am*-PNAs.** The doubly modified cationic *am*-PNAs were tagged with carboxy fluorescein (*cf*P4, *cf*P7, and *cf*P10) for evaluating their ability to enter living cells via flow cytometry and determine their subcellular

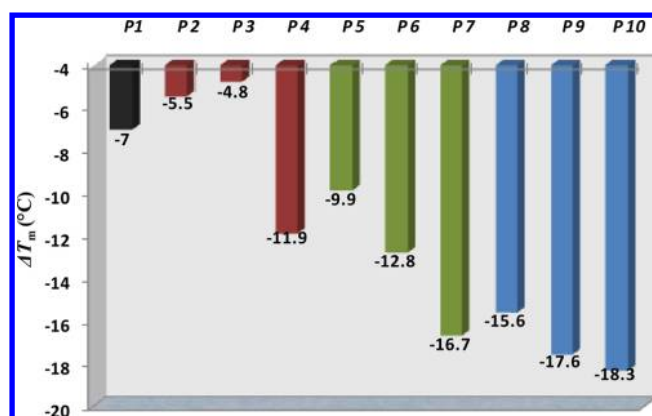


**Figure 4.** Comparative  $\Delta T_m$  values of *aeg* PNA P1 and *am*-PNAs P2–P10 with base pair C:C mismatch DNA3.

localization by fluorescent microscopic techniques. For the cellular uptake assay, a monolayer of HeLa cancer cells was incubated with each fluorescently labeled PNA (1  $\mu$ M), and after 24 h of incubation, the medium-containing *cf am*-PNAs was aspirated for gentle fixing of cells. The distribution of fluorescence was examined by fluorescence microscopy with 60 $\times$  objective. Figure 5 shows images of untreated cells after DAPI staining (Figure 5B) and *cf am*-PNA treated cells (Figure 5C) and the superimposed images (Figure 5D). It is seen that both unmodified PNA *cf*P1 and the cationic PNAs *cf*P4, *cf*P7, and *cf*P10 are localized in the nucleus (just like DAPI) even at the lowest of concentrations studied (0.25  $\mu$ M). The results indicate that although all PNAs could enter the nucleus, the true regio ( $\alpha/\gamma$ ) or stereo (*R/S*) effects of the modified cationic *am*-PNAs could not be distinguished. This was done by flow cytometry analysis.

HeLa cells were cultured in complete media and incubated individually with fluorescently labeled PNA for 24 h. After incubation, the cells were briefly washed with PBS buffer and analyzed by flow cytometry. The experiments were done at two different temperatures of 4 and 37 °C, and the results are shown in Figure 6. The different mean fluorescence seen for various *am*-PNAs shows differences in uptake properties. At 4 °C, only modest uptake efficiency is observed for unmodified *cf*P1 and  $\alpha$ -(*S-am*) PNA *cf*P4, both having similar mean fluorescence values (Figure 6, x-axis). A significant increase in the cell uptake was observed for  $\alpha$ -(*R-am*) PNA *cf*P7 followed by  $\gamma$ -*am*-PNA *cf*P10, which had 10–100 times higher uptake efficiency at 4 °C. However, there was no difference in the number of cells that uptake different PNAs, since the number of events (y-axis) remained the same for all PNAs. The corresponding results at a higher temperature (37 °C) indicated that the number of cells that uptake the *am*-PNAs almost doubled up, while the mean fluorescence decreased. These data suggest that the (i)  $\gamma$ -*am*-PNA *cf*P10 is taken up by the cells better than the unmodified PNA *cf*P1 and  $\alpha$ -(*R/S-am*) PNAs *cf*P7/*cf*P4 and (ii) the cell uptake is a function of both regio- ( $\gamma > \alpha$ ) and stereochemical (*R > S*) properties of *am*-PNAs.

**Cell Viability Assay.** In order to test the cellular toxicity of different *am*-PNAs, MTT assay was carried out on HeLa cells incubated with *am*-PNAs at various concentrations (0.1–5  $\mu$ M) in a humidified 5% CO<sub>2</sub> atmosphere. The assays were run in triplicate, and the percent viability of cells was determined using standard protocol. The cytotoxicity profiles (Figure 7) indicate that the viability of cells treated with *am*-PNAs is more than

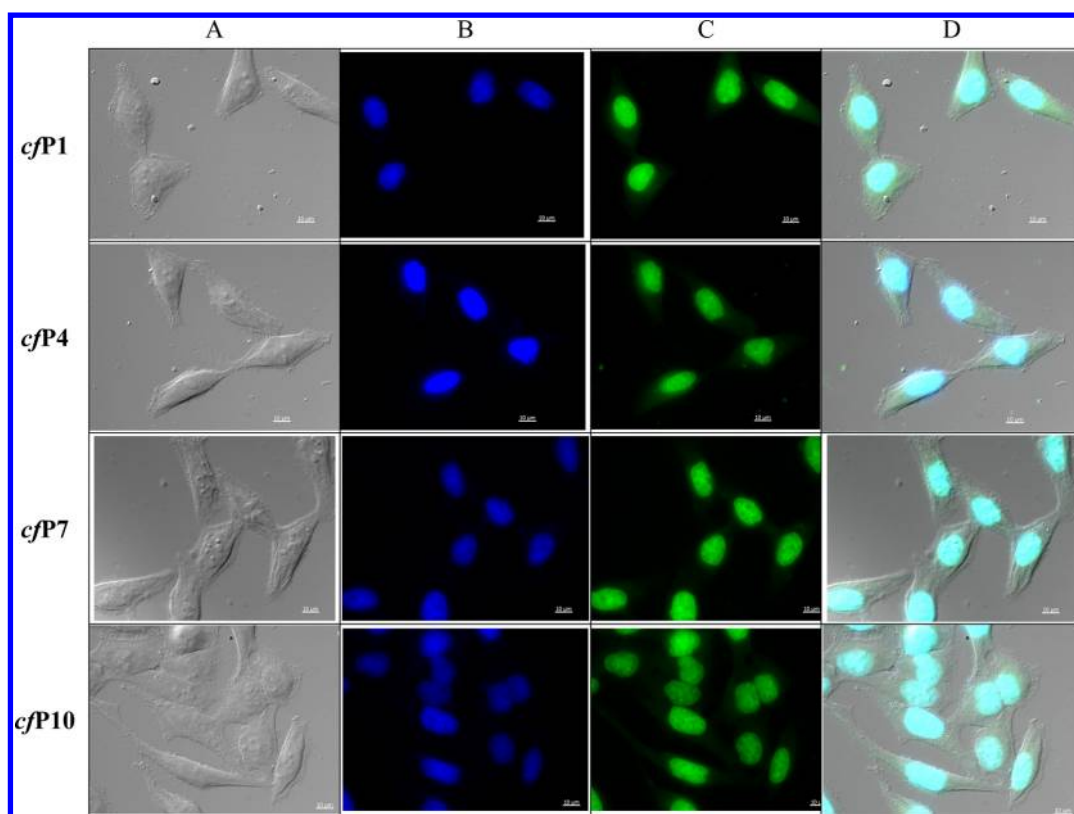


**Figure 5.** Nuclear localization of *am*-PNAs in HeLa cells: (A) DIC image, (B) DAPI stained image, (C) fluorescent image, and (D) superimposed image of (B) and (C).

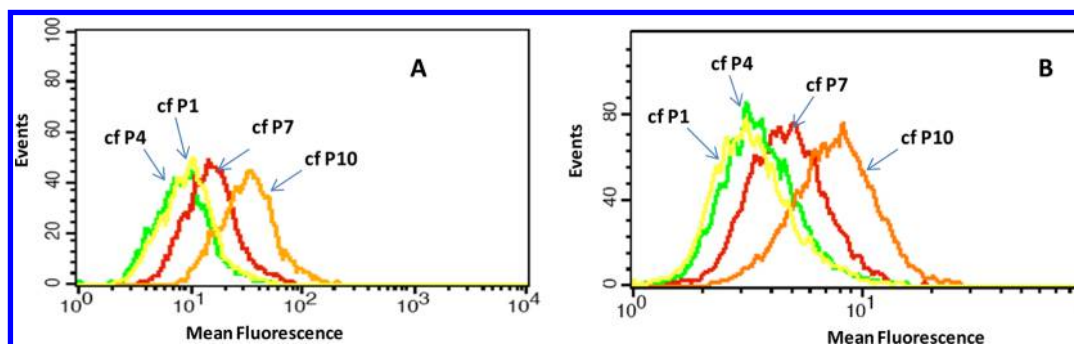


**Figure 6.** FACS analysis of HeLa cells incubated with *cf* PNAs ( $1 \mu\text{M}$ , 24 h) at (A)  $4 \text{ }^\circ\text{C}$  and (B)  $37 \text{ }^\circ\text{C}$ .

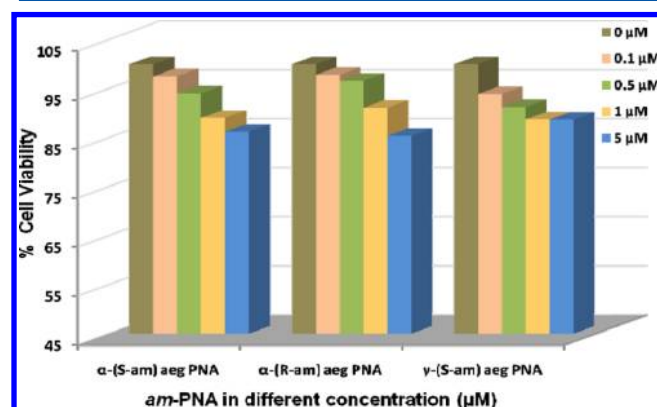


**Figure 7.** Dosage-dependent cytotoxicity profile of PNA oligomers on the basis of MTT assay. The cell viability is represented as the percent of viable HeLa cells incubated with 0, 0.1, 0.5, 1, and  $2 \mu\text{M}$  concentrations of indicated oligomers at  $37 \text{ }^\circ\text{C}$ .

85% even at the highest concentration of  $5 \mu\text{M}$ . Although no significant differences were seen among the different *am*-PNAs, within the experimental limits, the  $\gamma$ -(*S-am*)-PNA was found to show minimal toxicity at  $5 \mu\text{M}$ . These data indicate that the *am*-PNAs are favorably safe for use as potential therapeutic agents.

**Discussion.** On the basis of the reported observation that the *D*-lysine-substituted PNA backbone stabilizes the derived PNA:DNA hybrids and the theoretical studies of Topham et al.<sup>16</sup> suggesting intramolecular H-bonding of  $\alpha$ -methyleneamine side chain with the amide carbonyl of PNA backbone, *am*-PNA-T monomers having an *R/S*-methyleneamine substituent at the  $\alpha$ -C (**8a/b**) and *S*-substituent at  $\gamma$ -C (**16**) were synthesized. The synthesis was started from *D/L*-asparagine by reducing either the side-chain amide or the  $\alpha$ -carboxyl function to generate the desired cationic methyleneamine side chain. These were incorporated into *am*-PNA oligomers **P2–P10** corresponding to mixed base PNA sequences having single or double modifications at C-/N-terminus and in the middle for

studying their complexation with cDNA in parallel and antiparallel manner. It was seen that (i) the cationic *am*-PNAs stabilized the derived PNA:DNA hybrids compared to the unmodified PNA, (ii) the stability increased with the number of substitutions, and (iii) the antiparallel duplexes were more stable than the corresponding parallel duplexes. The degree of stability was in the order  $\gamma(S) > \alpha(R) > \alpha(S)$ . The reason for enhanced stability was not due to mere backbone electrostatic interaction of cationic PNA with anionic DNA, since even a single C:C mismatch in PNA:DNA hybrids resulted in increased destabilization of hybrids from the *am*-PNAs compared to that of unmodified PNA:DNA hybrid. The cationic *am*-PNA designs possess shorter aliphatic side chains compared to D-lysine-based PNA and hence may be less prone to engage in nonspecific electrostatic interactions with nucleotide phosphate groups of DNA molecules. The chiral center created on PNA backbone may favorably preorganize the PNA to generate hybridization competent conformations. This is reflected in the CD profile of  $\gamma$ -(*S-am*) PNA in single stranded form, which showed negative band of significant intensity, which was absent in the CD of  $\alpha$ -(*R/S-am*) PNA. This may be a consequence of a better stacking of bases arising from conformational preorganization of the backbone induced by specific chiral center at C- $\gamma$ . It is also reflected in the higher  $T_m$  of  $\gamma$ -(*S-am*) PNA:DNA hybrids which was about 6.5 °C per modification compared to 2.5–3.0 °C per modification for  $\alpha$ -(*R/S-am*) PNAs and 2 °C per modification for earlier reported  $\gamma$ -guanidino-PNAs.<sup>23</sup>

It is noteworthy that the cationic *am*-PNAs also transverse the cell membrane of HeLa cells and localize into the nucleus as shown by the fluorescent-labeled *am*-PNAs (Figure 5) in their superimposed images with DAPI stained cells. Quantitative differences among the different *am*-PNAs were obtained by the flow cytometry experimental data obtained at two different temperatures. As seen from the fluorescence, the cells take the  $\gamma$ -(*S-am*)-PNAs better than the  $\alpha$ -*am* PNAs with the *R*-stereomer better than the *S*-isomer. At a higher temperature, the number of cells taking up the PNAs increased suggesting that the cell uptake mechanism could be energy dependent, while the accompanying decreased fluorescence may be a consequence of quenching. The observed cell viability of more than 85% in MTT assay, even at a higher concentration of 5  $\mu$ M pointed to the low toxicity of *am*-PNAs, enabling the possibility of safe delivery into cells.

**Conclusions.** We have comprehensively demonstrated that the chiral, cationic *am*-PNAs containing a short aminomethylene side chain on the *aeg* PNA backbone at either the  $\alpha$  or  $\gamma$  position stabilize hybrid duplexes with cDNA in a regio- and stereospecific manner. The higher binding of cationic *am*-PNAs is associated with stringent base specificity as seen from severe destabilization in single mismatch duplexes, and the antiparallel duplexes are more stable than parallel duplexes. The *am*-PNA modifications are shown to improve the cellular uptake and get localized in nucleus of HeLa cells to which they are nontoxic. The studies represent a systematic analysis of regio and stereospecific effects of PNA modifications on cDNA binding, cell uptake and toxicity effects, with the  $\gamma$ (*S*)-substituted *am*-PNA performing superior to  $\alpha$ -substituted (*R/S*)-PNA and the *R*-isomer better than *S*-isomer in the latter case. Such data is of value in tuning the PNA modifications to desired properties. These inherently cationic and intrinsically chiral PNAs are thus promising for applications in therapeutics and the  $\gamma$ -*S-am*-PNA has a good potential for construction of

suitable target sequences to take them to the next stage of biological testing for antisense activity.

## EXPERIMENTAL SECTION

All of the starting materials were used without purification. Other details are given in the Supporting Information.

***N $\alpha$* -Boc-L-diaminopropionic Acid (2a).** A slurry of Boc-L-asparagine (5.0 g, 21.5 mmol) in ethyl acetate (24 mL), acetonitrile (24 mL), water (12 mL), and iodosobenzene diacetate (8.32 g, 25.8 mmol) was cooled and stirred at 16 °C for 30 min. The temperature was raised to 20 °C, and the reaction was stirred until completion (~4 h). The reaction mixture was cooled to 0 °C and filtered under vacuum. The filter cake was washed with ethyl acetate and dried in vacuo at 65 °C to obtain **2a** (3.88 g, 88% yield): mp 205–212 °C;  $[\alpha]_D^{25} +7.32$  (*c* 0.527, MeOH); IR (KBr)  $\nu$  (cm<sup>-1</sup>) 3528, 3507, 3349, 3033–2581, 2968, 1688, 1660, 1534, 1461, 1404, 1364, 1016 cm<sup>-1</sup>; <sup>1</sup>H NMR (200 MHz, MeOH-*d*)  $\delta_H$  7.81–7.77 (m, 1H), 7.25–7.17 (m, 1H), 4.17–4.11 (m, 1H), 3.25–3.22 (m, 2H), 1.54 (s, 9H) ppm; ESI-MS (*m/z*) calcd 204.1110, obsd 205.2667 [*M*<sup>+</sup> + *H*], 227.2656 [*M* + *Na*]<sup>+</sup>.

***N $\alpha$* -Boc-D-diaminopropionic acid (2b).** This compound was prepared from Boc-D-asparagine (**1b**) using the similar procedure as for **2a**. mp 202–208 °C.  $[\alpha]_D^{25} -8.88$ , (*c* 0.225, MeOH). IR (KBr)  $\nu$  (cm<sup>-1</sup>) 3528, 3507, 3349, 3033–2581, 2968, 1688, 1660, 1534, 1461, 1404, 1364, 1016 cm<sup>-1</sup>. <sup>1</sup>H NMR (200 MHz, MeOH-*d*)  $\delta_H$  7.81–7.77 (m, 1H), 7.25–7.17 (m, 1H), 4.17–4.11 (m, 1H), 3.25–3.22 (m, 2H), 1.54 (s, 9H) ppm. ESI-MS (*m/z*) calcd 204.1110, obsd 205.2675 [*M*<sup>+</sup> + *H*], 227.2938 [*M* + *Na*]<sup>+</sup>.

***N $\alpha$* -Boc-N $\beta$ -Cbz-amino-L-alanine (3a).** To an ice-cold stirred solution of **2a** (330 mg, 1.6 mmol) in water (3.3 mL) was added NaHCO<sub>3</sub> (340 mg, 4 mmol) slowly in portions. To this mixture was added CbzCl (330 mg, 1.9 mmol, 0.7 mL of a 50% solution in toluene) in one stretch and the resulting mixture stirred vigorously for 8 h at ambient temperature. Toluene was removed under reduced pressure, and the aqueous layer was washed with ether (10 mL  $\times$  2). The ethereal layer was discarded, and the aqueous layer was acidified to pH 2 with citric acid. The compound was extracted into ethyl acetate, and the organic phase washings were pooled together, washed with brine, dried over anhydrous Na<sub>2</sub>SO<sub>4</sub>, and then concentrated to obtain **3a** as a sticky oil (370 mg, 67% yield):  $[\alpha]_D^{25} +8.4$  (*c* 0.24, MeOH); <sup>1</sup>H NMR (200 MHz, CDCl<sub>3</sub>)  $\delta_H$  7.25 (s, 5H), 5.80–5.69 (br, 1H), 5.05 (s, 2H), 4.34 (s, 1H), 3.56 (m, 2H), 1.40 (s, 9H) ppm; <sup>13</sup>C NMR (200 MHz, CDCl<sub>3</sub>)  $\delta_C$  173.3, 157.2, 155.8, 136.1, 128.3, 127.8, 80.0, 66.8, 54.1, 42.5, 28.1 ppm; ESI-MS (*m/z*) calcd 338.1478, obsd 339.2566 [*M* + *H*]<sup>+</sup>, 361.2721 [*M* + *Na*]<sup>+</sup>.

***N $\alpha$* -Boc-N $\beta$ -Cbz-amino-D-alanine (3b).** This compound was prepared from **2b** using a similar procedure as for **3a**. It was isolated in the form of white solid compound: mp 78.5–81.3 °C;  $[\alpha]_D^{25} -7.6$  (*c* 0.43, MeOH); <sup>1</sup>H NMR (200 MHz, CDCl<sub>3</sub>)  $\delta_H$  7.32 (s, 5H), 6.24 (b, 1H), 5.96 (b, 1H), 5.09 (s, 2H), 4.39 (m, 1H), 3.64 (m, 2H), 1.43 (s, 9H) ppm; <sup>13</sup>C NMR (200 MHz, CDCl<sub>3</sub>)  $\delta_C$  173.3, 157.2, 155.8, 136.1, 128.3, 127.8, 80.0, 66.8, 54.1, 42.5, 28.1 ppm; ESI-MS (*m/z*) calcd 338.1478, obsd 339.25 [*M* + *H*]<sup>+</sup>, 361.27 [*M* + *Na*]<sup>+</sup>.

***N $\alpha$* -Boc- $\beta$ -Cbz-amino-L-alanine Methyl Ester (4a).** To a cold solution of **3a** (5.1 g, 15 mmol) in DMF (50 mL) was added activated K<sub>2</sub>CO<sub>3</sub> (2.3 g, 16 mmol). After the solution was stirred for 15 min in an ice–water bath, MeI (3.8 mL, 59 mmol) was added to the white suspension and stirring was continued at rt for 8 h at which point TLC analysis indicated complete formation of methyl ester. The solvent was removed from the reaction mixture, and the residue was partitioned between ethyl acetate (15 mL) and water (15 mL). The organic phase was washed with brine, dried with MgSO<sub>4</sub>, filtered, and concentrated. The residue was purified on silica gel using light petroleum and ethyl acetate to afford **4a** as a pale amber oil which on subsequent cooling solidified into a shiny white compound (3.8 g, 71.4% yield): mp 38–43 °C;  $[\alpha]_D^{25} +25.64$  (*c* 1.092, CHCl<sub>3</sub>); <sup>1</sup>H NMR (200 MHz, CDCl<sub>3</sub>)  $\delta_H$  7.25 (s, 5H), 5.41 (b, 1H), 5.14 (b, 1H), 5.08 (s, 2H), 4.34 (b, 1H), 3.72 (s, 3H), 3.58 (t, 2H), 1.42 (s, 9H) ppm; <sup>13</sup>C NMR (200 MHz, CDCl<sub>3</sub>)  $\delta_C$  173.3, 157.2, 155.8, 136.1, 128.3, 127.8, 80.0, 66.8, 54.1,

42.5, 28.1 ppm; ESI-MS ( $m/z$ ) calcd 352.1634, obsd 353.50  $[M + H]^+$ , 375.5088  $[M + Na]^+$ , 391.5032  $[M + K]^+$ .

**$\alpha$ -Boc- $N\beta$ -Cbz-amino-D-alanine Methyl Ester (4b).** Compound 4b was prepared from 3b using a similar procedure as for 4a: mp 42–46.4 °C;  $[\alpha]_D^{25} -24.13$  (c 0.663,  $CHCl_3$ );  $^1H$  NMR (200 MHz,  $CDCl_3$ )  $\delta_H$  7.25 (s, 5H), 5.47 (b, 1H), 5.20 (b, 1H), 5.07 (s, 2H), 4.35 (b, 1H), 3.72 (s, 3H), 3.57 (m, 2H), 1.42 (s, 9H) ppm;  $^{13}C$  NMR (200 MHz,  $CDCl_3$ )  $\delta_C$  173.3, 157.2, 155.8, 136.1, 128.3, 127.8, 80.0, 66.8, 54.1, 42.5, 28.1 ppm; ESI-MS ( $m/z$ ) calcd 352.1634, obsd 375.0083  $[M + Na]^+$ , 390.9739  $[M + K]^+$ .

**$N$ -(2-Boc-aminoethyl)- $N$ -(3-Cbz-amino-L-alanyl) Methyl Ester (5a).** Compound 4a (500 mg) was dissolved in DCM (1 mL), and TFA (1 mL) was added at 0 °C. The mixture was stirred for 1 h. Toluene (5 mL) was added, and volatiles were removed under vacuum. After sufficient removal of volatiles, the TFA salt of the compound (760 mg) was obtained as a crude oil. Without further purification, this residue was dissolved in methanol (10 mL), and Boc-aminoacetaldehyde (248 mg, 1.6 mmol) diluted in MeOH (2.5 mL) was added with continuous stirring at 0 °C. DIPEA (0.7 mL, 4.3 mmol) was added to this stirred solution dropwise very slowly. After the mixture was stirred for 30 min, glacial acetic acid (0.2 mL) and  $NaCNBH_3$  (134 mg, 2.1 mmol) were added sequentially. The reaction mixture was stirred for 3 h. All volatiles were removed under vacuum, and the residue was dissolved in ethyl acetate and extracted with saturated aqueous  $NaHCO_3$ . The organic phase, after drying with  $MgSO_4$ , was removed under vacuum, and the residue was purified by flash chromatography eluting with ethyl acetate–petroleum ether. Compound 5a was obtained as a yellow oil (470 mg, 83.8% yield):  $[\alpha]_D^{25} +3.23$  (c 0.5,  $CHCl_3$ );  $^1H$  NMR (200 MHz,  $CDCl_3$ )  $\delta_H$  7.34 (m, 5H), 5.28 (b, 1H), 5.09 (s, 2H), 4.91 (b, 1H), 3.71 (s, 3H), 3.49 (m, 1H), 3.34 (m, 2H), 3.16 (m, 2H), 2.75–2.58 (m, 2H), 1.42 (s, 9H) ppm;  $^{13}C$  NMR (200 MHz,  $CDCl_3$ )  $\delta_C$  173.5, 156.5, 156.1, 136.4, 128.5, 128.5, 79.3, 66.9, 60.6, 52.3, 47.5, 42.8, 40.5, 28.4 ppm; ESI-MS ( $m/z$ ) calcd 395.2056, obsd 396.1504  $[M + H]^+$ , 418.0625  $[M + Na]^+$ .

**$N$ -(2-Boc-aminoethyl)- $N$ -(3-Cbz-amino-D-alanyl) Methyl Ester (5b).** This compound was prepared from 4b using a similar procedure as for 5a:  $[\alpha]_D^{25} -3.46$  (c 0.578,  $CHCl_3$ );  $^1H$  NMR (200 MHz,  $CDCl_3$ )  $\delta_H$  7.33 (m, 5H), 5.34 (b, 1H), 5.08 (s, 2H), 4.95 (b, 1H), 3.71 (s, 3H), 3.48 (m, 1H), 3.35 (m, 2H), 3.16 (m, 2H), 2.75–2.59 (m, 2H), 1.41 (s, 9H) ppm;  $^{13}C$  NMR (200 MHz,  $CDCl_3$ )  $\delta_C$  172.7, 155.8, 155.5, 135.6, 127.7, 127.4, 78.6, 66.1, 59.8, 51.5, 46.7, 42.0, 39.6, 27.6 ppm; ESI-MS ( $m/z$ ) calcd 395.2056, obsd 396.5209  $[M + H]^+$ , 418.5118  $[M + Na]^+$ .

**$N$ -(2-Boc-aminoethyl)- $N$ -(chloroacetyl)- $N$ -(3-Cbz-amino-L-alanyl) Methyl Ester (6a).** To a stirred solution of 5a (2.8 g, 7 mmol) in DCM (30 mL) and  $Et_3N$  (3.9 mL, 28 mmol) cooled to 0 °C was added chloroacetyl chloride (0.7 mL, 9.1 mmol). After 30 min, DCM was removed under reduced pressure, and the residue was extracted with DCM (2  $\times$  20 mL) followed by drying under  $Na_2SO_4$ . The solvent was evaporated under reduced pressure, and the residue was purified with column chromatography (petroleum ether/ethyl acetate) to afford chloro compound 6a as a yellow oil (2.546 g, 77% yield):  $[\alpha]_D^{25} -12.35$  (c 0.648,  $CHCl_3$ );  $^1H$  NMR (200 MHz,  $CDCl_3$ )  $\delta_H$  7.33 (s, 5H), 5.37 (b, 1H), 5.15–4.98 (q, 2H), 4.03 (m, 2H), 3.83 (m, 2H), 3.74 (s, 3H), 3.57 (m, 2H), 3.31 (m, 1H), 3.18 (m, 2H), 1.42 (s, 9H) ppm;  $^{13}C$  NMR (200 MHz,  $CDCl_3$ )  $\delta_C$  170.2, 167.6, 156.8, 156.1, 136.3, 128.5, 128.2, 80.0, 67.0, 60.4, 52.7, 49.9, 41.2, 40.0, 38.6, 28.3 ppm; ESI-MS ( $m/z$ ) calcd 471.1772, obsd 494.3328  $[M + Na]^+$ .

**$N$ -(2-Boc-aminoethyl)- $N$ -(chloroacetyl)- $N$ -(3-Cbz-amino-D-alanyl) Methyl Ester (6b).** This compound was prepared from 5b using a similar procedure as for 6a:  $[\alpha]_D^{25} +14.8$  (c 0.135,  $CHCl_3$ );  $^1H$  NMR (200 MHz,  $CDCl_3$ )  $\delta_H$  7.34 (s, 5H), 5.39 (b, 1H), 5.28 (b, 1H), 5.16–4.99 (q, 2H), 4.03 (m, 2H), 3.83 (m, 2H), 3.75 (s, 3H), 3.57 (m, 2H), 3.29 (m, 1H), 3.18 (m, 2H), 1.42 (s, 9H) ppm;  $^{13}C$  NMR (200 MHz,  $CDCl_3$ )  $\delta_C$  170.2, 167.6, 156.7, 156.2, 136.2, 128.6, 128.2, 80.0, 67.0, 60.4, 52.7, 49.9, 41.1, 40.0, 38.6, 28.4 ppm; ESI-MS ( $m/z$ ) calcd 471.1772, obsd 472.5432  $[M + H]^+$ , 494.5393  $[M + Na]^+$ .

**$N$ -(2-Boc-aminoethyl)- $N$ -(thymine-1-acetyl)- $N$ -(3-Cbz-amino-L-alanyl) Methyl Ester (7a).** A mixture of thymine (685 mg, 5.4 mmol) and anhydrous  $K_2CO_3$  (750 mg, 5.4 mmol) in dry DMF (25

mL) under nitrogen conditions was heated at 65 °C with continuous stirring for 1.5 h. The mixture was allowed to come to room temperature and then kept in an ice bath. To this was added dropwise 6a (2.3 mg, 4.9 mmol) diluted in DMF (15 mL). The reaction mixture was stirred for 8 h. DMF was removed under vacuum, and the residue was partitioned between ethyl acetate and water. The organic phase was washed with brine, dried with  $MgSO_4$ , filtered, and concentrated. The residue was purified on silica gel using light petroleum and ethyl acetate to afford 7a as a foamy solid (2.2 g, 78% yield): mp 69–72 °C;  $^1H$  NMR (200 MHz,  $CDCl_3$ )  $\delta_H$  9.19 (s, 1H), 7.33 (s, 5H), 6.86 (s, 1H), 5.79 (m, 1H), 5.54 (m, 1H), 5.09–5.06 (q, 2H), 4.72–4.64 (maj) (d, 1H), 4.19–4.11 (min) (d, 1H), 3.88–3.79 (m, 2H), 3.72 (s, 3H), 3.54 (m, 2H), 3.34 (m, 1H), 3.18–3.13 (m, 2H), 1.87 (s, 3H), 1.43 (s, 9H) ppm;  $^{13}C$  NMR (200 MHz,  $CDCl_3$ )  $\delta_C$  170.1, 167.3, 164.5, 156.9, 156.1, 151.4, 140.9, 136.5, 128.5, 128.2 ppm; ESI-MS ( $m/z$ ) calcd 561.2435, obsd 599.9580  $[M + K]^+$ .

**$N$ -(2-Boc-aminoethyl)- $N$ -(thymine-1-acetyl)- $N$ -(3-Cbz-amino-D-alanyl) Methyl Ester (7b).** This compound was prepared from 6b using a similar procedure as for 7a: mp 70–79 °C;  $^1H$  NMR (200 MHz,  $CDCl_3$ )  $\delta_H$  9.44 (s, 1H), 7.33 (s, 5H), 6.86 (bs, 1H), 5.88 (m, 1H), 5.57 (m, 1H), 5.15–5.00 (q, 2H), 4.72–4.64 (maj) (d, 1H), 4.19–4.12 (min) (d, 1H), 3.88 (m, 2H), 3.72 (s, 3H), 3.57 (m, 2H), 3.33 (m, 1H), 3.18 (m, 2H), 1.86 (s, 3H), 1.42 (s, 9H) ppm;  $^{13}C$  NMR (200 MHz,  $CDCl_3$ )  $\delta_C$  170.4, 167.6, 164.8, 157.2, 156.4, 151.6, 141.2, 136.8, 128.8, 128.5, 111.2, 80.2, 67.1, 61.3, 53.0, 49.7, 48.8, 39.9, 39.1, 28.7, 12.7 ppm; ESI-MS ( $m/z$ ) calcd 561.2435, obsd 562.3598  $[M + 1]^+$ , 584.3475  $[M + Na]^+$ .

**$N$ -(2-Boc-aminoethyl)- $N$ -(thymine-1-ylacetyl)- $N$ -(3-Cbz-amino-L-alanine) (8a).** To compound 7a suspended in THF was added a solution of 0.5 M LiOH in water, and the mixture was stirred for 30 min. THF was removed under vacuum, and the aqueous layer was washed with DCM. The aqueous layer was then neutralized with activated Dowex  $H^+$  resin until the pH of the solution turned 4.0–5.0. The resin was removed by filtration, and the filtrate was concentrated to obtain the resulting Boc-protected monomer 8a in excellent yield (>85%):  $^1H$  NMR (200 MHz,  $CDCl_3$ )  $\delta_H$  7.39 (m, 5H), 7.28 (bs, 1H), 5.13 (s, 2H), 4.73–4.65 (maj) (d, 1H), 4.52–4.44 (min) (d, 1H), 4.09–4.01 (t, 1H), 3.76–3.73 (d, 2H), 3.55–3.42 (m, 2H), 3.30–3.29 (m, 2H), 1.9 (s, 3H), 1.49 (s, 9H); ESI-MS ( $m/z$ ) calcd 547.2278, obsd 585.9543  $[M + K]^+$ .

**$N$ -(2-Boc-aminoethyl)- $N$ -(thymine-1-ylacetyl)- $N$ -(3-Cbz-amino-D-alanine) (8b).** The hydrolysis procedure as described for compound 8a was followed to afford 8b in good yield:  $^1H$  NMR (200 MHz, MeOD)  $\delta_H$  7.39 (m, 5H), 7.29 (bs, 1H), 5.13 (s, 2H), 4.73–4.65 (maj) (d, 1H), 4.52–4.43 (min) (d, 1H), 4.09–4.01 (t, 1H), 3.78–3.74 (d, 2H), 3.36 (m, 2H), 3.30 (m, 2H), 1.9 (s, 3H), 1.49 (s, 9H) ppm; ESI-MS ( $m/z$ ) calcd 547.2278, obsd 570.5063  $[M + Na]^+$ , 586.4932  $[M + K]^+$ .

**$\alpha$ -Boc- $N\beta$ -Cbz-aminoalaninol (9).** To an ice-cooled solvent mixture of dry THF (15 mL) and absolute ethanol (10 mL) containing  $NaBH_4$  (269 mg, 7.1 mmol) in a three necked flask was slowly added LiBr (617 mg, 7.1 mmol) for ~30 min. The above solution was stirred for 1.0 h, and the appearance of turbid milky solution indicated the formation of  $LiBH_4$  in situ. To the above ice-cooled solution was added 4a (500 mg, 1.4 mmol) from a dropping funnel over a period of 30 min under  $N_2$  atmosphere, and the reaction mixture was stirred overnight at rt. The pH was then adjusted to 7.0 by addition of a saturated solution of  $NH_4Cl$ . The solvent mixture was removed under vacuum, and the residue was extracted into ethyl acetate (10 mL  $\times$  3). The organic layer was washed with water followed by brine solution, dried over anhydrous  $Na_2SO_4$ , and concentrated to afford a white shiny solid product 9 (360 mg, 78% yield,  $R_f = 0.65$ , ethyl acetate: petroleum ether 1:1): mp 77.2–80.2 °C;  $[\alpha]_D^{25} +12.6$  (c 0.317,  $CHCl_3$ );  $^1H$  NMR (200 MHz,  $CDCl_3$ )  $\delta_H$  7.33 (s, 5H), 5.45 (b, 1H), 5.17 (b, 1H), 5.09 (s, 2H), 3.63 (m, 2H), 3.54 (m, 1H), 3.30 (m, 2H), 1.40 (s, 9H) ppm;  $^{13}C$  NMR (200 MHz,  $CDCl_3$ )  $\delta_C$  158.0, 156.0, 136.1, 128.6, 128.1, 79.8, 67.2, 61.7, 52.2, 41.1, 28.3 ppm; ESI-MS ( $m/z$ ) calcd 324.1685, obsd 325.2679  $[M + H]^+$ , 347.2411  $[M + Na]^+$ .

***N* $\alpha$ -Boc-*N* $\beta$ -Cbz-aminoalanine Methyl Sulfonate (10).** Compound **9** (0.3 g, 0.7 mmol) was dissolved in dry DCM (5 mL) and cooled to 0 °C. Et<sub>3</sub>N (0.3 mL, 2 mmol) was added dropwise and the mixture stirred for the next 10 min. To this ice-cooled solution was added freshly distilled mesyl chloride (0.1 mL, 1 mmol) from a dropping funnel over a period of 10 min under N<sub>2</sub> atmosphere. The reaction mixture was stirred for 30 min. DCM was removed under reduced pressure, and the residue was extracted into ethyl acetate (5 mL  $\times$  2), washed with water, dried over Na<sub>2</sub>SO<sub>4</sub>, and concentrated to yield almost pure (single spot on TLC) sticky mesylate derivative **10** (0.20 g, 90% crude yield, *R*<sub>f</sub> = 0.7, ethyl acetate/petroleum ether 1:1) which was immediately used in the next step without further purification.

**(S)-Benzyl tert-Butyl (3-Azidopropane-1,2-diyl)dicarbamate (11).** To the solution of **10** (152 mg, 0.4 mmol) in DMF (2 mL) was added NaN<sub>3</sub> (350 mg, 5.4 mmol). The reaction mixture was stirred at 55 °C for 8 h. The solvent was removed under reduced pressure, and the residue was extracted into ethyl acetate (5 mL  $\times$  3). The combined organic layer was washed with brine, dried over anhydrous Na<sub>2</sub>SO<sub>4</sub>, and then concentrated to yield **11** (104 mg, 83% yield *R*<sub>f</sub> = 0.3; 40% ethyl acetate/petroleum ether): mp 105.8–106.9 °C; [ $\alpha$ ]<sub>D</sub><sup>25</sup> -6.17 (c 0.324, CHCl<sub>3</sub>); IR (CHCl<sub>3</sub>)  $\nu$  (cm<sup>-1</sup>) 3440.22, 3019.66, 2957.18, 2927.72, 2856.13, 2400.76, 2106.59, 1712.59, 1514.91, 1455.80, 1368.47, 1215.60, 1163.85, 1064.64, 755.63 cm<sup>-1</sup>; <sup>1</sup>H NMR (200 MHz, CDCl<sub>3</sub>)  $\delta$ <sub>H</sub> 7.33 (s, 5H), 5.20 (b, 1H), 5.09 (s, 2H), 3.78 (m, 1H), 3.45–3.42 (d, 2H), 3.35–3.29 (t, 2H), 1.42 (s, 9H) ppm; <sup>13</sup>C NMR (200 MHz, CDCl<sub>3</sub>)  $\delta$ <sub>C</sub> 157.1, 155.6, 136.2, 128.5, 128.1, 80.0, 67.0, 52.2, 50.6, 42.6, 28.2 ppm; ESI-MS (*m/z*) calcd 349.1750, obsd 350.1430 [M + H]<sup>+</sup>, 372.1436 [M + Na]<sup>+</sup>.

**(R)-Benzyl tert-Butyl (3-Aminopropane-1,2-diyl)dicarbamate (12).** To a solution of **11** (100 mg) in MeOH (10 mL) taken in a hydrogenation flask was added Raney nickel (5 mL). The reaction mixture was hydrogenated in a Parr apparatus for 3.5 h at rt and H<sub>2</sub> pressure of 35–30 psi. The catalyst was filtered off, and the solvent was removed under reduced pressure to yield a residue of compound **12** as a colorless oil (65 mg, 61% yield). This compound was used for the next reaction without any further purification.

**$\gamma$ -am-(Cbz)-PNA Backbone Ethyl Ester (13).** Compound **12** (0.05 g, 0.2 mmol) was treated with ethyl bromoacetate (15.5  $\mu$ L, 0.14 mmol) in acetonitrile (1 mL) in the presence of Et<sub>3</sub>N (65  $\mu$ L, 0.5 mmol), and the mixture was stirred at ambient temperature for 5 h. The solid that separated was removed by filtration, and the filtrate was evaporated to obtain the alkylated derivative **13** (0.05 g, 79% yield; *R*<sub>f</sub> = 0.63, 70% EtOAc/petroleum ether) as a colorless oil: <sup>1</sup>H NMR (200 MHz, CDCl<sub>3</sub>)  $\delta$ <sub>H</sub> 7.33 (s, 5H), 5.50 (b, 1H), 5.26 (b, 1H), 5.08 (s, 2H), 4.21–4.11 (q, 2H), 3.70–3.60 (m, 1H), 3.37 (s, 2H), 3.32–3.19 (m, 2H), 2.80–2.57 (m, 2H), 1.41 (s, 9H), 1.25 (t, 3H) ppm; <sup>13</sup>C NMR (200 MHz, CDCl<sub>3</sub>)  $\delta$ <sub>C</sub> 172.4, 157.1, 156.1, 136.5, 128.5, 128.1, 79.7, 66.8, 60.9, 50.9, 50.3, 43.4, 28.4, 14.2 ppm; ESI-MS (*m/z*) calcd 409.2213, obsd 410.4282 [M + H]<sup>+</sup>.

**$\gamma$ -am-(Cbz)-(N-chloroacetyl)-PNA Backbone Ethyl Ester (14).** Compound **13** (500 mg, 1.2 mmol) was dissolved in DCM (5 mL) under ice-cooled conditions, and Et<sub>3</sub>N (0.7 mL, 4.8 mmol) was added. The reaction mixture was stirred for a few minutes, and then chloroacetyl chloride (0.1 mL, 1.6 mmol) was added dropwise with vigorous stirring. The reaction was complete within 0.5 h. The compound was partitioned between the organic layer and aqueous phase, and the product was extracted into the organic phase. It was then purified on silica gel using column chromatography technique to obtain **14** as colorless oil in good yield (400 mg, 67.4% yield; *R*<sub>f</sub> = 0.6; 40% EtOAc/petroleum ether): <sup>1</sup>H NMR (200 MHz, CDCl<sub>3</sub>)  $\delta$ <sub>H</sub> 7.32 (s, 5H), 5.89 (b, 1H), 5.47 (b, 1H), 5.15–5.01 (q, 2H), 4.27–4.23 (m, 1H), 4.20–4.14 (m, 2H), 3.96 (s, 2H), 3.81–3.61 (m, 2H), 3.45–3.34 (m, 2H), 3.15–2.96 (m, 2H), 1.40 (s, 9H), 1.28–1.25 (t, 3H) ppm; <sup>13</sup>C NMR (200 MHz, CDCl<sub>3</sub>)  $\delta$ <sub>C</sub> 169.0, 168.6, 157.7, 155.8, 136.4, 128.5, 128.1, 79.7, 66.9, 62.2, 61.5, 51.1, 50.5, 50.3, 41.0, 28.3, 14.1 ppm; ESI-MS (*m/z*) calcd 485.1929, obsd 486.2656 [M + H]<sup>+</sup>, 508.3486 [M + Na]<sup>+</sup>.

**$\gamma$ -am-(Cbz)-(N-thymine-1-ylacetyl)-PNA Backbone Ethyl Ester (15).** A mixture of **14** (1 g, 2 mmol), thymine (286 mg, 26

mmol) and anhydrous K<sub>2</sub>CO<sub>3</sub> (313 mg, 26 mmol) in dry DMF (10 mL) under N<sub>2</sub> atmosphere was heated with stirring at 65 °C for 5 h. After cooling, the solvent was removed under reduced pressure to leave a residue, which was extracted into DCM (2  $\times$  25 mL) and dried over Na<sub>2</sub>SO<sub>4</sub>. The solvent was evaporated, and the crude compound was purified by column chromatography (MeOH/DCM) to afford a pale white solid of **15** (935 mg, 79% yield, *R*<sub>f</sub> = 0.8, 80% EtOAc/petroleum ether): mp 141.9–144.1 °C; <sup>1</sup>H NMR (400 MHz, CDCl<sub>3</sub>)  $\delta$ <sub>H</sub> 10.10 (maj) and 9.70 (min) (s, 1H), 7.31 (s, 5H), 7.02 (maj) and 6.95 (min) (br s, 1H), 6.30 (maj) and 6.07 (min) (br s, 1H), 5.88 (maj) and 5.61 (min) (br s, 1H), 5.13–5.01 (m, 2H), 4.40–4.32 (m, 2H), 4.25–4.22 (q, 2H), 4.16–4.11 (m, 1H), 3.91–3.75 (m, 2H), 3.58 (m, 2H), 3.40 (m, 2H), 1.87 (s, 3H), 1.40 (maj) and 1.33 (min) (s, 9H), 1.24–1.20 (t, 3H) ppm; <sup>13</sup>C NMR (400 MHz, CDCl<sub>3</sub>)  $\delta$ <sub>C</sub> 169.3 (maj) and 169.1 (min), 168.7 (maj) and 167.5 (min), 164.5, 157.8, 156.0 (min) and 155.8 (maj), 151.8 (min) and 151.3 (maj), 141.4 (min) and 141.0 (maj), 136.5 (min) and 136.3 (maj), 128.5, 128.1, 111.0, 79.8, 66.9, 62.4, 61.5, 50.5, 48.0, 41.5, 28.4, 14.1, 12.3 ppm; ESI-MS (*m/z*) calcd 575.2591, obsd 576.4506 [M + H]<sup>+</sup>, 598.4256 [M + Na]<sup>+</sup>.

**$\gamma$ -am-(Cbz)-(N-thymine-1-ylacetyl)-PNA Monomer (16).** The usual hydrolysis procedure as described for compound **8** was followed to afford the monomer **16** in good yield: <sup>1</sup>H NMR (200 MHz, DMSO)  $\delta$ <sub>H</sub> 11.34 (br s, 1H), 7.36 (s, 5H), 6.93 (maj) and 6.69 (min) (s, 1H), 5.06 (s, 2H), 4.75–4.47 (m, 2H), 4.16 (m, 1H), 4.0–3.85 (m, 2H), 3.53–3.34 (m, 2H), 3.15 (m, 2H), 1.77 (s, 3H), 1.38 (s, 9H) ppm; ESI-MS (*m/z*) calcd 547.2278, obsd 548.4579 [M + H]<sup>+</sup>, 570.4857 [M + Na]<sup>+</sup>.

**Circular Dichroism.** CD spectra were recorded on CD spectropolarimeter. The CD spectra of the PNA:DNA complexes and the relevant single strands were recorded in 10 mM sodium phosphate buffer, 10 mM NaCl (pH 7.2) as an accumulation of five scans from 300 to 190 nm using a 1 cm cell, a resolution of 0.1 nm, a bandwidth of 1.0 nm, sensitivity of 2 m deg, response of 2 s, and a scan speed of 50 nm/min. The concentration of the samples was calculated on the basis of absorbance from the molar extinction coefficients of the corresponding nucleobases (i.e., T = 8.8 cm<sup>2</sup>/μmol; C = 7.3 cm<sup>2</sup>/μmol; G = 11.7 cm<sup>2</sup>/μmol, and A = 15.4 cm<sup>2</sup>/μmol). The samples were annealed by keeping the samples at 90 °C for 5 min followed by slow cooling to room temperature. Then the samples were cooled by keeping at 4 °C overnight. The CD spectra of all the samples were recorded at 10 °C in the range 190–300 nm. The ellipticity value was plotted as a function of the PNA mole fraction at 256 nm.

**Job's Plot.** For the binding stoichiometry determination, 11 mixtures of PNA:DNA with different ratios to each other such as 0:100, 10:90, 20:80, 30:70, 40:60, 50:50, 60:40, 70:30, 80:20, 90:10, and 100:0; all of the same total strand concentration (2 μM) in sodium phosphate buffer (10 mM NaCl, pH 7.2). The samples were annealed, and their CD spectra were recorded at 10 °C at the range 190–300 nm. The ellipticity value was plotted as a function of the PNA mole fraction at 256 nm where the CD plots show an isodichroic point at around 260–265 nm. The ellipticity values of all the mixtures at 262 nm (for P3) and 266 nm (for P4) are plotted against mole fraction of PNA. The ellipticity of PNA readily increases, reaches a maximum, and then again decreases. The stoichiometry of the paired strands was obtained from the intersecting point of this mixing curve, in which the optical property at a given wavelength was plotted as a function of mole fractions of each strand. The data were processed using Microcal Origin 6.0.

Absorbance spectra at 260 nm were also recorded for the mixtures of PNA:DNA in different proportions as mentioned above. A mixing curve was plotted and absorbance at fixed wavelength ( $\lambda_{\text{max}}$  260 nm) against mole fractions of PNA. The minimum of intersect corresponds to the binding stoichiometric molar ratio.

**UV-T<sub>m</sub> measurements.** The complexes were prepared in 10 mM sodium phosphate buffer, pH 7.2 containing NaCl (10 mM). Absorbance versus temperature profiles were obtained by monitoring at 260 nm with a UV spectrophotometer equipped with a temperature programmer and water circulator, scanning from 10 to 85 °C with temperature increments of 0.5 °C per minute. The data were

processed using Microcal Origin 6.0 and  $T_m$  values derived from the derivative curves.

**Fluorescence Microscopy.** HeLa cells were maintained at 37 °C in a humidified atmosphere containing 5% CO<sub>2</sub> in D-MEM containing 2 mM L-glutamine, 10% FBS, and 4 µg/L gentamycin solution. They were allowed to grow for the next 24 h, after which time the culture medium containing PNA was discarded. The cells were washed twice with PHEM buffer (60 mM Pipes, 25 mM Hepes, 10 mM EGTA, 2 mM MgCl<sub>2</sub>·6H<sub>2</sub>O; pH 6.9) for 10 min at room temperature and then gently fixed for 10 min using 3.5% paraformaldehyde and 0.05% glutaraldehyde in PHEM buffer as the fixing agent. After fixation, the cells were washed thoroughly three more times for 10 min with PHEM. The coverslips were then mounted using mounting medium that comprised of 90% glycerol, 0.5% N-propyl gallate (or propyl 3,4,5-trihydroxybenzoate) and 20 mM Tris-Cl (pH 8.0) containing 0.0004 mg/mL of DAPI (or 4', 6-diamidino-2-phenylindole) on objective glass slides. The distribution of fluorescence was examined by fluorescence microscopy on with 60× objective. Micrographs were viewed and analyzed using AXIO-VISION software. Images were acquired with the same camera settings for all cells with PNAs.

**Flow Cytometry Analysis.** All the PNA oligomers (cf PNAs; labeled with carboxyfluorescein) were evaluated for cellular uptake using flow cytometry. The cells were seeded into 60 mM plates at a density of 1–2 × 10<sup>6</sup>/dish in 3 mL media and grown in a humidified 5% CO<sub>2</sub> atmosphere at 4 and 37 °C. The cells were then incubated with the fluorescently labeled PNA oligomers at 1 µM for 24 h. Following incubation, the cell suspension was centrifuged at 300g. The cell pellet was washed twice with 1 × PBS (pH 7.4) at 300xg for 5 min. Cells were washed once more with PBS and were finally resuspended in PBS (500 µL). For each experiment, a control of cells that were not incubated with PNA was also analyzed. The samples were run in triplicate and each experiment was repeated twice within the same week. Fluorescence analysis for both the live cell lines was performed with Flow Cytometer using FL1 laser for excitation of carboxyfluorescein at 488 nm. Cell Quest software was used to analyze the data. A minimum of 20000 events per sample was analyzed.

**Cell Viability Assay.** To determine the cellular toxicity of the am-PNAs, they were assessed using the 3-(4,5-dimethylthiazol-2-yl)-2,5-diphenyltetrazolium bromide (MTT) cell viability experiment. HeLa cells used for this purpose were grown in a humidified 5% CO<sub>2</sub> atmosphere at 37 °C for 48 h. The cells were seeded into 96-well plates at a density of 50000 cells/mL in a medium containing D-MEM (high glucose), 2 mM L-glutamine, 4 µg/L of gentamycin antibiotic solution, and 10% heat-inactivated FBS. For the assay, 10 µL of 5 mg/mL of MTT solution was added in each well containing a cell monolayer having various concentrations of am-PNAs in 100 µL culture medium in dark. For each experiment, a control of cells which were not incubated with PNAs was also analyzed. Plates were incubated at 37 °C for 4 h, followed by removal of MTT/media solution. The precipitated crystals were dissolved in 100 µL of DMSO and the solution absorbance was read at 570 nm using Flash multimode plate reader.

## ■ ASSOCIATED CONTENT

### ■ Supporting Information

<sup>1</sup>H and <sup>13</sup>C NMR spectra of compounds 2–16; HPLC and MALDI-TOF of PNA P1–P10 and fluorescent PNA cfP1, cfP4, cfP7, and cfP10; UV–Jobs plot, CD–Jobs plot, and UV–melting profile of various modified PNA:DNA duplexes; UV–absorbance spectra and fluorescence emission spectra. This material is available free of charge via the Internet at <http://pubs.acs.org>.

## ■ AUTHOR INFORMATION

### Corresponding Author

\*Tel: 91 (20) 2590 8021. Fax: 91 (20) 2589 9790. E-mail: [kn.ganesh@iiserpune.ac.in](mailto:kn.ganesh@iiserpune.ac.in).

## Notes

The authors declare no competing financial interest.

## ■ ACKNOWLEDGMENTS

R.M. acknowledges UGC India for the award of a fellowship. K.N.G. thanks DST, New Delhi, for the J. C. Bose Fellowship.

## ■ REFERENCES

- (1) Nielsen, P. E.; Egholm, M.; Berg, R. H.; Buchardt, O. *Science* **1991**, *254*, 1497–1500.
- (2) Egholm, M.; Buchardt, O.; Nielsen, P. E.; Berg, R. H. *J. Am. Chem. Soc.* **1992**, *114*, 1895–1897.
- (3) Nielsen, P. E. *Acc. Chem. Res.* **1999**, *32*, 624–630.
- (4) Egholm, M.; Buchardt, O.; Christensen, L.; Behrens, C.; Frier, S. M.; Driver, D. A. *Nature* **1993**, *365*, 566–569.
- (5) Nielsen, P. E.; Egholm, M.; Berg, R. H.; Buchardt, O. *Anti-Cancer Drug Des.* **1993**, *8*, 53–63.
- (6) Boffa, L. C.; Morris, P. L.; Carpeneto, E. M.; Louissaint, M.; Allfrey, V. G. *J. Biol. Chem.* **1996**, *271*, 13228–13233.
- (7) Ray, A.; Norden, B. *FASEB* **2000**, *14*, 1041–1060.
- (8) Ganesh, K. N.; Nielsen, P. E. *Curr Org. Chem.* **2000**, *4*, 931–943.
- (9) Kumar, V. A.; Ganesh, K. N. *Acc. Chem. Res.* **2005**, *38*, 404–412.
- (10) Kumar, V. A.; Ganesh, K. N. *Curr Top Med Chem.* **2007**, *7*, 715–726.
- (11) Haaima, G.; Lohse, A.; Buchardt, O.; Nielsen, P. E. *Angew Chem., Int. Ed.* **1996**, *35*, 1939–1942.
- (12) Sforza, S.; Corradini, R.; Ghirardi, S.; Dossena, A.; Marchelli, R. *Eur. J. Org. Chem.* **2000**, 2905–2913.
- (13) Tedeschi, T.; Sforza, S.; Dossena, A.; Corradini, R.; Marchelli, R. *Chirality* **2005**, *17*, 196–204.
- (14) Dragulescu-Andrasi, A.; Zhou, P.; He, G.; Ly, D. H. *Chem. Commun.* **2005**, 244–246.
- (15) Menchise, V.; De Simone, G.; Tedeschi, T.; Corradini, R.; Sforza, S.; Marchelli, R.; Capasso, D.; Saviano, M.; Pedone, C. *Proc. Natl. Acad. Sci. U.S.A.* **2003**, *100*, 12021–12026.
- (16) Topham, C. M.; Smith, J. C. *Biophys. J.* **2007**, *92*, 769–786.
- (17) Mitra, R.; Ganesh, K. N. *Chem Comm.* **2011**, *47*, 1198–1200.
- (18) Kleiner, R.; Brudno, Y.; Birnbaum, M. E.; Liu, D. *J. Am. Chem. Soc.* **2008**, *130* (14), 4646–4659.
- (19) Englund, E. A.; Appella, D. H. *Org. Lett.* **2005**, *7*, 3465–3467.
- (20) Dose, C.; Seitz, O. *Org. Lett.* **2005**, *7*, 4365–4368.
- (21) Tedeschi, T.; Sforza, S.; Corradini, R.; Marchelli, R. *Tetrahedron Lett.* **2005**, *46*, 8395–8399.
- (22) Dragulescu-Andrasi, A.; Rapireddy, S.; Frezza, B. M.; Gayathri, C.; Gil, R. R.; Ly, D. L. *J. Am. Chem. Soc.* **2006**, *128*, 10258–10267.
- (23) Sahu, B.; Chenna, V.; Lathrop, K. L.; Thomas, S. M.; Zon, G.; Livak, K. J.; Ly, D. H. *J. Org. Chem.* **2009**, *74*, 1509–1516.
- (24) Sahu, B.; Sacui, I.; Rapireddy, S.; Zanotti, K. J.; Bahal, B.; Armitage, B. A.; Ly, D. H. *J. Org. Chem.* **2011**, *76*, 5614–5627.
- (25) Zhang, L.; Kauffman, G. S.; Pesti, J. A.; Yin, J. *J. Org. Chem.* **1997**, *62*, 6918–6920.
- (26) Delaet, N. G. J.; Robinson, L. A.; Wilson, D. M.; Sullivan, R. W.; Bradley, E. K.; Dankwardt, S. M.; Martin, R. L.; Van Wart, H. E.; Walker, K. A. M. *Bioorg. Med. Chem. Lett.* **2003**, *13*, 2101–2104.
- (27) Dueholm, K. L.; Egholm, M.; Buchardt, O. *Org. Prep. Proced. Int* **1993**, *25*, 457–461.
- (28) Dale, J. A.; Mosher, H. S. *J. Am. Chem. Soc.* **1973**, *95*, 512–519.
- (29) Seco, J. M.; Quinoa, E.; Riguera, R. *Chem. Rev.* **2004**, *104*, 17–117.